JB
Journals.ASM.org

Dual Mechanisms of Metabolite Acquisition by the Obligate Intracytosolic Pathogen *Rickettsia prowazekii* Reveal Novel Aspects of Triose Phosphate Transport

Kyla M. Frohlich,* Jonathon P. Audia

Laboratory of Molecular Biology, Department of Microbiology and Immunology, University of South Alabama College of Medicine, Mobile, Alabama, USA

***Rickettsia prowazekii* is an obligate intracytosolic pathogen and the causative agent of epidemic typhus fever in humans. As an evolutionary model of intracellular pathogenesis, rickettsiae are notorious for their use of transport systems that parasitize eukaryotic host cell biochemical pathways. Rickettsial transport systems for substrates found only in eukaryotic cell cytoplasm are uncommon among free-living microorganisms and often possess distinctive mechanisms. We previously reported that *R. prowazekii* acquires triose phosphates for phospholipid biosynthesis via the coordinated activities of a novel dihydroxyacetone phosphate transport system and an *sn*-glycerol-3-phosphate dehydrogenase (K. M. Frohlich et al., J. Bacteriol. 192:4281–4288, 2010). In the present study, we have determined that *R. prowazekii* utilizes a second, independent triose phosphate acquisition pathway whereby *sn*-glycerol-3-phosphate is directly transported and incorporated into phospholipids. Herein we describe the *sn*-glycerol-3-phosphate and dihydroxyacetone phosphate transport systems in isolated *R. prowazekii* with respect to kinetics, energy coupling, transport mechanisms, and substrate specificity. These data suggest the existence of multiple rickettsial triose phosphate transport systems. Furthermore, the *R. prowazekii* dihydroxyacetone phosphate transport systems displayed unexpected mechanistic properties compared to well-characterized triose phosphate transport systems from plant plastids. Questions regarding possible roles for dual-substrate acquisition pathways as metabolic virulence factors in the context of a pathogen undergoing reductive evolution are discussed.**

Rickettsia prowazekii is the causative agent of louse-borne typhus in humans and is designated a select agent. Members of the genus *Rickettsia* are Gram-negative alphaproteobacteria that grow only within the cytosol of a eukaryotic host cell (for reviews, see references 1 to 5). Rickettsiae are evolutionarily related to mitochondria (6) and present a fascinating biological paradigm—organisms that grow with cytoplasm on both sides of their cell membrane. Obligate intracytosolic growth is thought to be a primary driver of rickettsial genome reductive evolution, where many genes encoding *de novo* biosynthetic pathways have been lost (6–9). Instead, rickettsiae avail themselves of the metabolite pools of the host cell through the use of carrier-mediated transport systems (10–15). In essence, the eukaryotic host cell provides the metabolites that rickettsiae would otherwise have to synthesize themselves, thus creating a selective environment conducive to rickettsial genome reduction and metabolic streamlining (1). Conversely, environmental fluctuations, perturbations, and instabilities negate such a narrow strategy for the free-living microorganism, which has instead maintained coordinated, adaptive responses to furnish metabolic flexibility.

Despite the paring effects of reductive evolution, some rickettsial metabolic pathways have retained complexity. The classical example is the dual energy acquisition pathways that maintain rickettsial adenylate energy charge. *R. prowazekii* possesses an intact tricarboxylic acid cycle and an electron transport system (ETS) that generate a proton motive force (PMF) to drive ATP production via oxidative phosphorylation (6, 16). Rickettsiae also possess an ATP/ADP translocase (Tlc1), an obligate exchange antiporter that transports host cell ATP in a 1:1 exchange for rickettsial ADP and serves as a form of energy parasitism (11). These two adenylate energy charge maintenance systems are differentially regulated (17), but it remains unknown whether they act redundantly or if both are essential components of rickettsial metabolism.

Previously, we published a report describing the identification of an *sn*-glycerol-3-phosphate (G3P) dehydrogenase (G3PDH) that functions as part of a novel triose phosphate acquisition system in *R. prowazekii* (18). We determined that *R. prowazekii* acquires G3P for phospholipid biosynthesis, at least in part, by transporting dihydroxyacetone phosphate (DHAP) and catalyzing its conversion to G3P via the activity of G3PDH (encoded by the RP442 open reading frame). This observation explained the conservation of the *R. prowazekii* RP442 open reading frame, which might otherwise be considered an orphaned enzyme because its usual biochemical pathways, glycolysis and gluconeogenesis, are no longer present in the rickettsial metabolic repertoire. It appears that the selective pressure to maintain the G3PDH came as a consequence of the acquisition of a DHAP transport system and a perceived essential role for this pathway in rickettsial phospholipid biosynthesis.

Our previous studies discussed an obvious question of whether *R. prowazekii* might also possess transport systems for G3P to fuel phospholipid biosynthesis in addition to the DHAP/G3PDH system. Herein we describe the properties of the *R. prowazekii* G3P

Received 9 April 2013 **Accepted** 7 June 2013
Published ahead of print 14 June 2013
Address correspondence to Jonathon P. Audia, jaudia@southalabama.edu.
* Present address: Kyla M. Frohlich, The RNA Institute, University at Albany, Albany, New York, USA.

doi:10.1128/JB.00404-13

transport systems and their contribution to phospholipid synthesis. In addition, we describe the kinetic, energetic, mechanistic, and substrate specificity properties of the *R. prowazekii* G3P and DHAP transport pathways. On the basis of these data, we posit the existence of at least two separate triose phosphate transporters. Interestingly, the *R. prowazekii* DHAP transport systems displayed mechanistic properties that distinguish it from other known triose phosphate transport systems.

MATERIALS AND METHODS

Chemicals, media, and radiolabeled triose phosphate synthesis. Unless otherwise indicated, the chemicals and enzymes used in this study were from Sigma. [γ-^{32}P]ATP, $^{32}P_i$, and [^{14}C]glycerol were from PerkinElmer. [^{14}C]G3P was from American Radiochemicals. [^{32}P]G3P and [^{32}P]DHAP were synthesized as previously described (18).

Propagation and isolation of *R. prowazekii*. All of the experiments described in this report were performed with the Madrid E strain of *R. prowazekii* (chicken embryo yolk sac passage number 282) purified as described in reference 18. Purified rickettsiae were suspended in a solution containing 220 mM sucrose, 12 mM potassium phosphate, 4.9 mM potassium glutamate, and 10 mM magnesium chloride, pH 7.0 ($SPGMg^{2+}$), and the quality of the preparation was assessed by (i) a hemolysis endpoint assay to quantify metabolically active rickettsiae (19), (ii) ATP transport assays in the presence or absence of atractyloside to assess the separation of rickettsiae from contaminating mitochondria (11, 20), and (iii) lysine transport with and without the protonophore carbonyl cyanide *m*-chlorophenylhydrazone (CCCP) as a second measure of rickettsial preparation quality (10, 16). Selected rickettsial preparations were assayed for cytochrome *c* oxidase activity at different purification steps for both infected and mock-infected chicken embryo yolk sacs as a further control for mitochondrial contamination (11). For all rickettsial preparations, mitochondrial contamination was determined to be less than 5%.

Assays of G3P and DHAP transport kinetics. Purified rickettsiae were suspended in a modified $SPGMg^{2+}$ solution where the potassium phosphate concentration was changed to 1 mM. The phosphate was lowered to limit its potential effect as a competitive inhibitor of triose phosphate transport. Uptake of radiolabeled substrates was measured by the filtration-and-wash method (i.e., transport assay) previously described (18). Transport assays were initiated by the addition of 20 μM [^{14}C]G3P, 20 μM [^{32}P]G3P, or 10 μM [^{32}P]DHAP to the reaction mixture, and 0.1-ml aliquots were filtered and washed with time. As controls for the background caused by the transport of substrate breakdown products, purified rickettsiae were tested for transport of glycerol (20 μM supplemented with [^{14}C]glycerol at 0.5 μCi ml^{-1}) and inorganic phosphate (1 mM supplemented with $^{32}P_i$ at 0.5 μCi ml^{-1}). Kinetic data were collected during the initial linear rate of transport and determined by varying the substrate concentration from 0.5 to 800 μM. Inhibition profiles were determined by assaying G3P and DHAP transport in the presence of putative inhibitors added to the reaction mixture at a 20-fold excess over the estimated K_t (kinetic constant of transport, equivalent to the Michaelis constant, K_m) concentration of G3P or DHAP (see the legend to Fig. 5 for the compounds tested). All of the transport data were normalized to the amount (milligrams) of total *R. prowazekii* protein as determined with the Bio-Rad DC Protein Assay (in accordance with the manufacturer's directions).

Estimation of intracellular G3P concentration and analysis of *R. prowazekii* phospholipid biosynthesis. The rickettsial cytoplasmic concentration of [^{32}P]G3P and its incorporation into phospholipids by purified rickettsiae were determined as previously described for [^{32}P]DHAP (18).

Energetics of G3P and DHAP transport determined via poisoning assays. Energy coupling of rickettsial transport of G3P and DHAP was determined by pretreating rickettsiae with 1 mM potassium cyanide (KCN) or 10 μM CCCP. In separate reaction mixtures, KCN was combined with 20 μg ml^{-1} venturicidin, a poison that blocks the activity of the F_1F_0 ATP synthetase (ATPase) (21). All inhibitor combinations were added to the rickettsial suspension 10 min prior to the addition of radiolabeled substrate. To reverse the effects of KCN energy poisoning, 2.5 mM ATP (pH 7.4) was subsequently added 10 min after the addition of substrate. Addition of ATP rescues both the adenylate energy charge and the PMF in a Tlc1- and F_1F_0 ATPase-dependent manner as previously described for rickettsial lysine transport (10, 16). The addition of venturicidin blocks the F_1F_0 ATPase and thus blocks ATP-mediated restoration of the energy charge. The nature of CCCP-mediated uncoupling makes it refractory to reversal by exogenous ATP. In all cases, control assays with no inhibitors were carried out in parallel.

Mechanisms of G3P and DHAP transport determined via substrate efflux assays. Purified rickettsiae were suspended in modified $SPGMg^{2+}$ solution, and transport assays were initiated by the addition of 20 μM [^{14}C]G3P or 10 μM [^{32}P]DHAP for 10 min at 34°C, followed by a 250-fold dilution into a morpholinepropanesulfonic acid (MOPS)-modified buffer consisting of 220 mM sucrose, 4.9 mM potassium glutamate, 10 mM $MgCl_2$, and 50 mM MOPS, pH 7.4, with or without the potential countersubstrates (see the legend to Fig. 4). The phosphate was replaced with MOPS to control for the possibility that phosphate could act as a countersubstrate to stimulate obligate exchange antiport-mediated substrate efflux. To control for the other components of the efflux buffer, separate experiments were conducted where substrate-loaded rickettsiae were diluted in 100 mM MOPS, pH 7.4, to initiate efflux. At the time points indicated in the figures, 25 ml of the rickettsial suspension was analyzed by the filtration-and-wash method, thus giving a number of rickettsiae equivalent to that of the standard transport assay described above (and in reference 18). The previously described *R. prowazekii* transport systems for ATP (11, 22) and lysine (10) were tested as controls.

RESULTS

***R. prowazekii* G3P transport and metabolism.** Classical *R. prowazekii* metabolic studies (23, 24) and genome sequence analyses (6) indicate that rickettsial fatty acid and phospholipid biosynthetic pathways appear intact, yet rickettsiae lack glycolytic/gluconeogenic pathways required to supply G3P for *de novo* phospholipid biosynthesis (6). These observations raised the question of how rickettsiae acquire G3P (or other triose phosphates) for phospholipid biosynthesis, with transport from the host being an obvious source. We previously described an interesting twist on rickettsial triose phosphate acquisition by demonstrating that purified, isolated *R. prowazekii* was able to transport exogenously supplied DHAP, convert it to G3P via the activity of a rickettsial G3PDH, and subsequently incorporate G3P into phospholipids (18). In the present study, we expanded our analysis of *R. prowazekii* triose phosphate and phospholipid metabolism by examining the possibility that exogenous G3P itself is transported. Figure 1A shows that *R. prowazekii* purified from chicken embryo yolk sacs was able to transport exogenous [^{14}C]G3P from the transport assay reaction buffer, a reaction that equilibrated over time. Control experiments demonstrated that [^{14}C]glycerol was not readily transported by rickettsiae, thus confirming G3P as the transported substrate rather than transport of its breakdown product (Fig. 1A).

To estimate the concentration of G3P in the rickettsial cytoplasm after 10 min of transport, we used a previously described modification of the standard filter uptake assay (18). In this method, [^{32}P]G3P is used as the substrate and metabolism that occurs subsequent to transport is determined. In addition, we ruled out the possible contribution of spurious [^{32}P]G3P breakdown and transport of $^{32}P_i$ (data not shown; see reference 18). We determined that ~83% of the total ^{32}P radiolabel posttransport

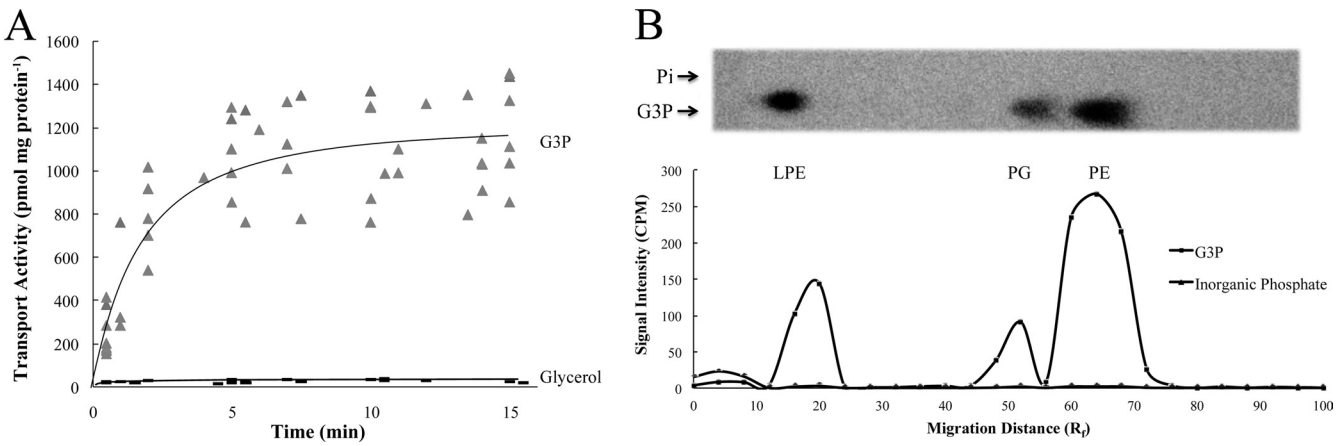

FIG 1 G3P transport and incorporation into phospholipids by purified *R. prowazekii*. (A) [^{14}C]G3P (20 μM) and [^{14}C]glycerol (20 μM) transport by purified *R. prowazekii* suspended in modified SPGMg^{2+} buffer was assayed at 34°C by filtration and washing. The data from different rickettsial preparations are plotted independently, and each point represents the average of technical triplicates. Experiments were performed with at least three independent rickettsial preparations for each time point. In all of the experiments, rickettsial hemolytic activity ranged between 3 and 8 optical density units (measured spectrophotometrically at 545 nm). Data are expressed as transport activity per milligram of total rickettsial protein. (B) Incorporation of [^{32}P]G3P into phospholipids was determined by incubating purified *R. prowazekii* suspended in modified SPGMg^{2+} buffer for 1 h (at 34°C), followed by organic extraction and thin-layer chromatographic analysis as previously described (18). As a control, we determined that $^{32}P_i$ (Pi) was not incorporated into phospholipids under identical conditions. The phosphorimage of a representative thin-layer chromatograph is shown along with a graphic representation of the data from three independent rickettsial preparations. The phosphorimage signal intensity (in counts per minute) was plotted for each substrate measured over 26 equal increments described as the migration distance relative to the mobile-phase front (R_f). Known standards were visualized by exposure to iodine vapor (not shown) to allow determination of the major radiolabeled species as lysophosphatidylethanolamine (LPE), phosphatidylglycerol (PG), and phosphatidylethanolamine (PE).

was recovered from the filtered and washed rickettsiae by ethanol extraction. This cytoplasmic, ethanol-soluble ^{32}P radiolabel was resolved by thin-layer chromatography, and the subsequent phosphorimaging analysis revealed that 82% ± 4% of the total ethanol-soluble radiolabel was present in a compound that migrated with a known G3P standard (mean value of at least three independent rickettsial preparations ± standard deviation). Furthermore, 10% ± 3% of the ethanol-soluble radiolabel migrated with an inorganic phosphate standard and 8% ± 2% migrated with an ATP standard. No detectable ^{32}P radiolabel corresponded to a DHAP standard, thus supporting our previous observation that the rickettsial G3PDH does not readily catalyze the conversion of G3P to DHAP (18).

By these chromatographic analyses, we determined that G3P transport after 10 min resulted in a concentration gradient of ~3.6-fold. Note that the rickettsial cytosolic water volume was determined as previously described (18, 25) and the intracellular G3P concentration was calculated by converting the thin-layer chromatographic data into an estimation of the molar amount of cytoplasmic [^{32}P]G3P (based on the known specific activity of the ^{32}P radiolabel). A concentration gradient of >1 indicates that rickettsial G3P uptake occurs via active, energy-dependent transport.

We further examined the downstream metabolism of transported G3P by assaying for its incorporation into rickettsial phospholipids. As anticipated (18), transported [^{32}P]G3P was incorporated by purified, isolated rickettsiae into organic soluble compounds that displayed migration patterns comparable to those of known phospholipid standards (analyzed by thin-layer chromatography and phosphorimaging; Fig. 1B). Determined as a percentage of the total organic-soluble ^{32}P radiolabel, the major phospholipid species corresponded to phosphatidylethanolamine (67% ± 3%), lysophosphatidylethanolamine (23% ± 4%), and phosphatidylglycerol (13% ± 4%). To discount the possibility that these incorporation data were due to [^{32}P]G3P breakdown, we determined that $^{32}P_i$ was not measurably incorporated into organic-soluble compounds (Fig. 1B). It is noteworthy that the observed [^{32}P]G3P incorporation profile corresponds to the known composition of *R. prowazekii* phospholipids determined in previous studies (23, 24). Taken together, these results indicate that *R. prowazekii* uses active, carrier-mediated substrate transport systems to take up G3P from the environment and metabolize it into membrane phospholipids.

Kinetics of *R. prowazekii* G3P and DHAP transport. Thus far, our past (18) and present studies suggest that *R. prowazekii* uses at least two different triose phosphate acquisition strategies. However, there is no information describing the kinetics and mechanisms of the G3P and DHAP transport systems. Figure 2A and B show Hanes-Woolf plots (initial substrate concentration/reaction velocity versus initial substrate concentration) of G3P and DHAP transport kinetic data, respectively. In this analysis, a linear relationship is indicative of a single transport system whereas a curvilinear pattern at low substrate concentrations is indicative of substrate recognition by more than one transport system. The curvilinear shape of the data plots in Fig. 2A and B as they approach the axis origin is highly reminiscent of the classical multitransport system kinetic relationship described for *Escherichia coli* amino acid transport (26). Thus, our data suggest the presence of more than one triose phosphate transport system responsible for the observed G3P and DHAP translocation by purified, isolated *R. prowazekii*.

Further comparison of G3P and DHAP transport kinetic data revealed a relatively high-velocity, low-affinity transport profile for G3P (apparent K_t, ~39 ± 7 μM; V_{max}, ~2.5 ± 0.5 pmol mg^{-1} min^{-1} [determined from Fig. 2A]) compared to the low-velocity, high-affinity transport profile observed for DHAP (apparent K_t,

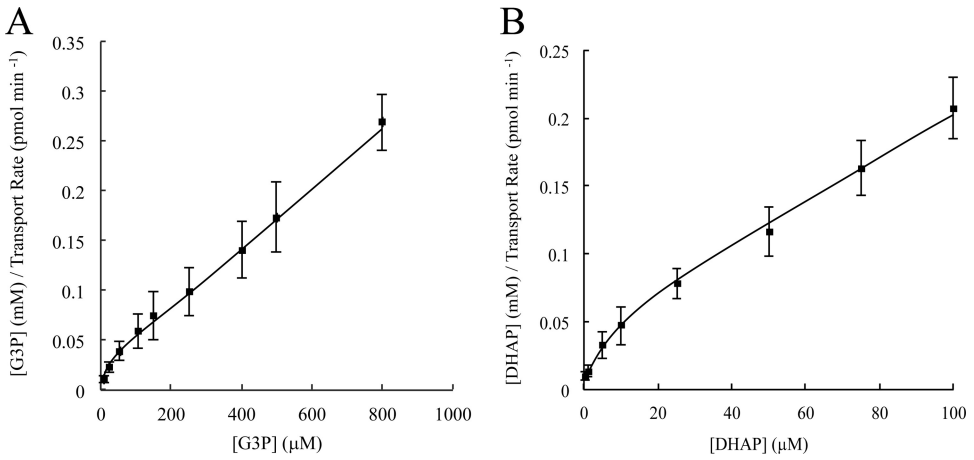

FIG 2 G3P and DHAP transport kinetics in purified *R. prowazekii*. Kinetic analysis of [^{14}C]G3P (A) and [^{32}P]DHAP (B) transport was performed with purified *R. prowazekii* suspended in modified SPGMg^{2+} buffer and assayed at 34°C over the indicated substrate concentration range. The initial linear transport rate was determined by filtration and washing. Hanes-Woolf kinetic plots are shown. Error bars represent standard deviations of the mean of at least three independent rickettsial preparations.

~6 ± 1.1 μM; V_{max}, ~0.4 ± 0.1 pmol mg^{-1} min^{-1} [determined from Fig. 2B]).

Energy dependence of *R. prowazekii* G3P and DHAP transport. On the basis of our observations that the *R. prowazekii* transport systems for G3P (above) and DHAP (18) are able to establish concentration gradients of >1, we examined transport energetics. To this end, poisons were used to investigate two of the predominant forms of energy coupling; namely, PMF and ATP dependence. Recall that rickettsiae possesses an ETS to generate PMF, which in turn is coupled to the generation of adenylate energy charge by the F_1F_0 ATPase. Thus, addition of KCN (an ETS complex IV inhibitor) destroys the PMF and consequently blocks ATP synthesis.

Studies of transport energetics with *R. prowazekii* are augmented by two powerful modifications of this classical approach. First, rickettsiae poisoned with KCN can be rescued via the activity of the ATP/ADP translocase Tlc1 (11). Addition of exogenous ATP to the transport assay reaction buffer stimulates Tlc1-dependent restoration of the adenylate energy charge, which in turn rescues PMF (i.e., the F_1F_0 ATPase runs in reverse by hydrolyzing ATP to drive proton extrusion and re-establish PMF) (16). Second, we describe a novel augmentation of this assay system that allows discrimination between ATP- and PMF-dependent energy coupling. Venturicidin is a poison that blocks the F_1F_0 ATPase (21). Thus, in the presence of both KCN and venturicidin, addition of exogenous ATP will restore the rickettsial adenylate energy charge only. By extension, exogenous ATP rescues transport systems that derive energy from ATP hydrolysis, whereas PMF-coupled transport systems are not rescued. Note that this approach does not discriminate between direct and secondary energy coupling (e.g., ATP hydrolysis establishes a concentration gradient of "compound X" that, in turn, is coupled to the establishment of a triose phosphate concentration gradient).

As a control, we used the uncoupler CCCP, a protonophore that allows protons to freely cross the lipid bilayer and dissipates PMF such that neither adenylate energy charge nor PMF can be rescued by the addition exogenous ATP.

Figure 3A validates the efficacy of this system by using [^{14}C]lysine uptake, which has been previously described as an *R. prowazekii* PMF-dependent transport system (10, 16). Addition of KCN at the start of the transport assay poisoned *R. prowazekii* [^{14}C]lysine transport (Fig. 3A, triangles, 0 to 9 min), and addition of exogenous ATP to the transport assay reaction buffer reversed the poisoning effects of KCN on [^{14}C]lysine transport (Fig. 3A, triangles, 10 to 25 min), as expected with a PMF-dependent transport system. Applying our augmented approach, we observed that the combination of KCN and venturicidin blocked the rescue of [^{14}C]lysine transport by ATP (Fig. 3A, squares). Addition of CCCP inhibited [^{14}C]lysine transport, and this inhibition cannot be reversed by the addition of ATP (Fig. 3A, circles).

Figure 3B shows that the addition of KCN at the start of the transport assay poisoned *R. prowazekii* [^{32}P]G3P transport (Fig. 3B, triangles, 0 to 9 min) and the addition of exogenous ATP to the transport assay reaction buffer reversed the poisoning effect of KCN on [^{32}P]G3P transport (Fig. 3B, triangles, 10 to 25 min). Interestingly, addition of ATP substantially reversed the effect of the combination of KCN and venturicidin, thus indicating the presence of an ATP-dependent G3P transport system and perhaps a minor PMF-dependent G3P transport system (Fig. 3B, squares). With the addition of CCCP, [^{32}P]G3P transport cannot be rescued by the addition of ATP (Fig. 3B, circles). These data also validate the observation that *R. prowazekii* requires energy to establish an ~3.6-fold G3P concentration gradient.

We previously determined that *R. prowazekii* establishes a DHAP concentration gradient (18). Figure 3C shows that addition of KCN at the start of the transport assay poisoned *R. prowazekii* [^{32}P]DHAP transport (Fig. 3C, triangles, 0 to 9 min) and addition of exogenous ATP to the transport assay reaction buffer resulted in modest reversal of the KCN poisoning effect (Fig. 3C, triangles, 10 to 25 min). This modest reversal raises the possibility of a direct inhibitory effect of KCN on the rickettsial DHAP transport system (testing of this idea will require identification of the DHAP transport system[s]). The combination of KCN and venturicidin prevented the modest reversal by ATP, suggestive of a PMF-dependent DHAP transport system (Fig. 3C, squares). As expected, the [^{32}P]DHAP transport system cannot be rescued by the addition of ATP when it is poisoned by CCCP (Fig. 3C, circles). Together, these observations suggest that *R. prowazekii* pos-

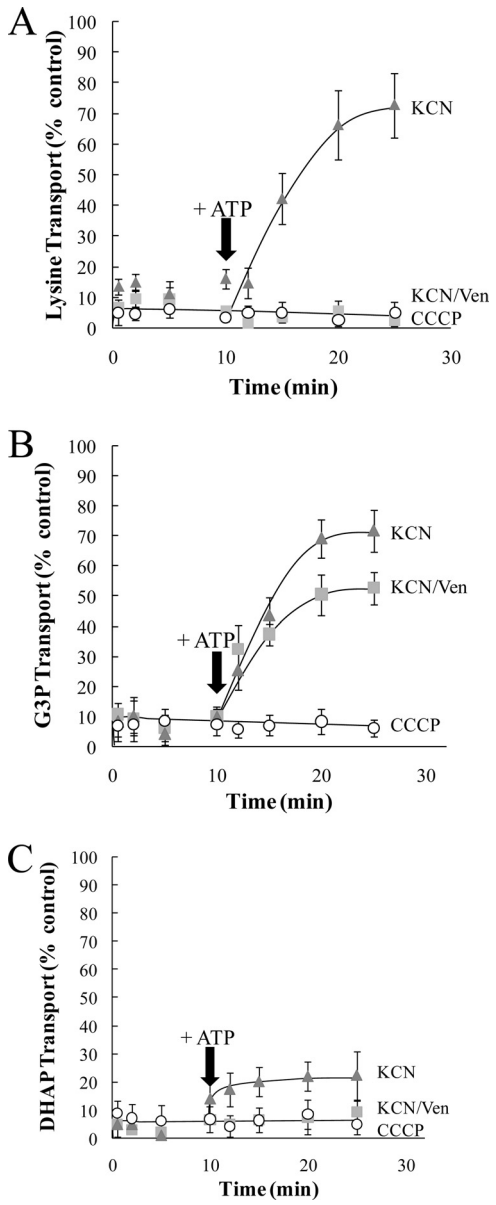

FIG 3 Energy poisoning inhibition and rescue analysis of G3P and DHAP transport in purified *R. prowazekii*. Transport assays were performed with purified *R. prowazekii* suspended in modified SPGMg^{2+} buffer at 34°C over a 25-min time course for [^{14}C]lysine (5 μM) (A), [^{14}C]G3P (20 μM) (B), or [^{32}P]DHAP (10 μM) (C). The inhibition data for each time point are presented as a percentage of the corresponding control (no energy poison) transport assay. Data points are the average of technical triplicates of at least three independent rickettsial preparations. Rickettsiae were preincubated for 10 min with CCCP (10 μM), KCN (1 mM), or a combination of KCN (1 mM) and venturicidin (Ven, 20 μg ml^{-1}), and transport assays were initiated by the addition of radiolabeled substrates. After 10 min of transport, ATP (2.5 mM) was added to the uptake mixture in an attempt to reverse the energy-poisoning effect (indicated with an arrow). The subsequent data points are presented as a percentage of the 10-min control (no energy poison) time point. In all cases, control assays with no inhibitors were carried out in parallel (data not shown). Error bars represent the standard deviations of the means.

sesses multiple G3P and DHAP active transport systems that establish concentration gradients in an energy-dependent fashion.

Mechanisms of *R. prowazekii* G3P and DHAP transport. Our observations regarding the energy dependence of the *R. prowazekii* DHAP transport systems have raised an interesting evolutionary contrast to other triose phosphate transport systems. For example, many bacteria and plant plastids encode triose phosphate transporters that require a one-to-one obligate counterexchange with inorganic phosphate; a mechanism referred to as obligate exchange antiport (27, 28). To determine if the *R. prowazekii* G3P and/or DHAP transport systems are driven by obligate exchange antiport, we employed a substrate efflux assay. Rickettsiae were first incubated with either [^{14}C]G3P or [^{32}P]DHAP to allow substrate transport and accumulation in the cytoplasm. The substrate-loaded rickettsiae were then diluted 250-fold and subsequently assayed by filtration washing over time. The dilution of the radiolabeled substrate renders it largely unavailable and effectively stops transport (influx) while also changing the substrate concentration gradient to favor the efflux of accumulated radiolabeled substrate from the rickettsial cytoplasm into the medium if it is possible. If substrate transport occurs via an obligate exchange antiport mechanism, then efflux will occur only when the radiolabeled substrate-loaded bacteria are diluted in medium containing the appropriate countersubstrate (11, 29). Figure 4A and B show control experiments validating the efflux profiles of previously described *R. prowazekii* transport systems for lysine (10) and ATP (11, 22). Rickettsiae loaded with [^{14}C]lysine (Fig. 4A, diamonds, 0 to 10 min) demonstrated substrate efflux upon dilution in transport assay buffer alone (Fig. 4A, squares, 12 to 25 min). Conversely, rickettsiae loaded with [^{32}P]ATP (Fig. 4B, diamonds, 0 to 10 min) did not display substrate efflux upon dilution in transport assay buffer alone (Fig. 4B, squares, 12 to 30 min) but [^{32}P]ATP did undergo efflux when an excess of unlabeled ATP was present in the transport assay buffer to serve as a countersubstrate (Fig. 4B, circles, 12 to 30 min). This is the expected profile of an obligate exchange antiport system.

Rickettsiae loaded with [^{14}C]G3P (Fig. 4C, diamonds, 0 to 10 min) showed substrate efflux upon dilution in medium (Fig. 4C, squares, 12 to 30 min). Interestingly, the addition of the unlabeled potential countersubstrate G3P (Fig. 4C, circles, 12 to 30 min) or inorganic phosphate (Fig. 4C, triangles, 12 to 30 min) appeared to modestly increase the rate of [^{14}C]G3P efflux from the rickettsial cytoplasm. Taken together with the kinetic data (Fig. 2B), these G3P efflux experiments suggest the possible existence of more than one transport system. The efflux profiles indicate that at least one of the G3P transport systems operates with an obligate exchange mechanism whereas the other(s) does not (Fig. 4A).

As an independent assessment of the transport mechanism, the energy poison KCN was added to the reaction mixture in lieu of the dilution step to stimulate efflux and dissipation of a substrate concentration gradient. Figure 4C shows that addition of KCN to rickettsiae loaded for 9 min with [^{14}C]G3P stimulated efflux (cross, 12 to 30 min) as expected.

Figure 4D demonstrates that, regardless of the composition of the diluent, [^{32}P]DHAP efflux occurred at a very low rate. Poisoning of the system with KCN to stimulate efflux resulted in a very similar low rate (cross, 12 to 30 min). We have previously determined by ethanol extraction and thin-layer chromatography that transported [^{32}P]DHAP in the rickettsial cytosol is not rapidly metabolized/trapped and thus should be available for efflux if it is possible (18). We also tested the possible unlabeled countersubstrates DHAP and inorganic phosphate over a range of increasing concentrations but did not observe any further stimulation of efflux (data not shown). Finally, we tested 100 mM MOPS buffer

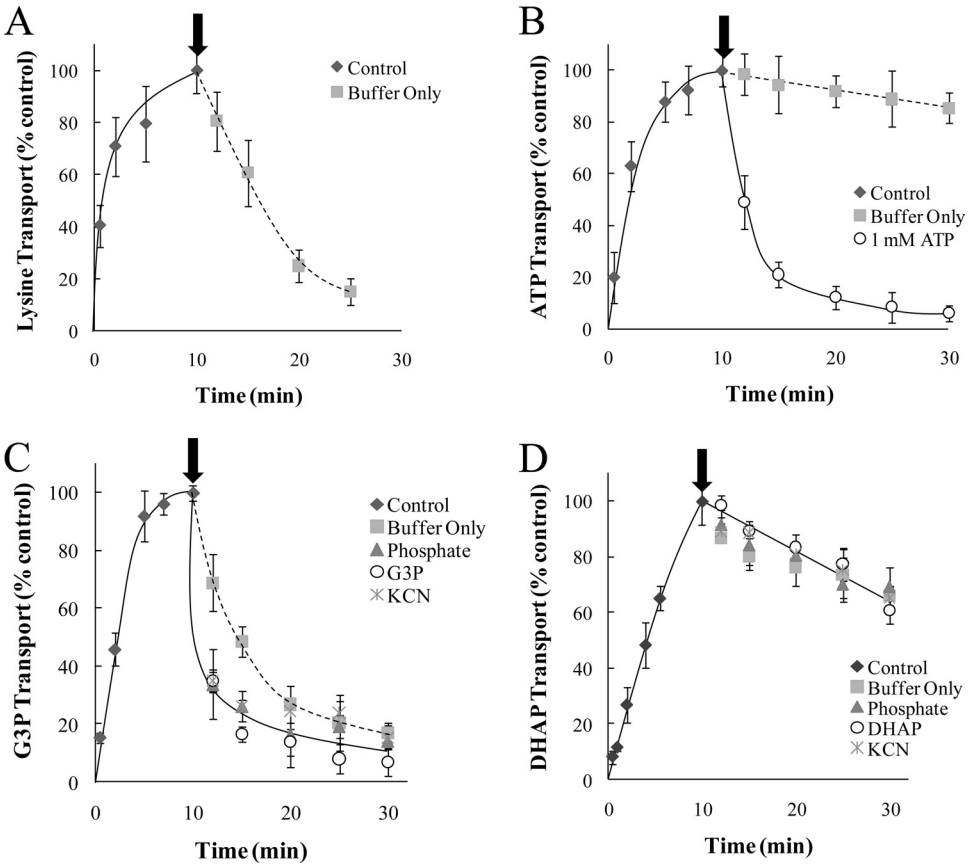

FIG 4 G3P and DHAP efflux profiles in purified *R. prowazekii*. Transport (0 to 10 min) and efflux (12 to 30 min) assays were performed with purified *R. prowazekii* suspended in modified SPGMg^{2+} buffer at 34°C for [^{14}C]lysine (5 μM) (A), [^{32}P]ATP (100 μM) (B), [^{14}C]G3P (20 μM) (C), or [^{32}P]DHAP (10 μM) (D). Data points are presented for each time point as a percentage of the 10-min control time point and are the average of technical triplicates of at least three independent rickettsial preparations. Transport assays (Control) were initiated by the addition of substrate, and efflux was initiated by 250-fold dilution at the 11-min time point (indicated with the arrow). The diluent was a MOPS-modified buffer alone (Buffer Only) or MOPS-modified buffer containing a potential countersubstrate. The candidate countersubstrates tested included phosphate, G3P, DHAP, and ATP (each at 1 mM), as indicated. As an independent method to test substrate efflux, the addition of KCN (1 mM) was substituted for the dilution step at the 10-min time point. Error bars represent the standard deviations of the means.

(pH 7.4) as a minimalistic diluent and generated the same efflux profile, suggesting that none of the components of the transport and efflux buffer were affecting the movement of DHAP (data not shown). Together, these data suggest that DHAP transport occurs via a uniport mechanism where the substrate moves through the carrier in one direction only.

Substrate specificity of *R. prowazekii* G3P and DHAP transport. To further characterize the *R. prowazekii* G3P and DHAP transport systems, we generated a substrate specificity profile. The standard uptake assay was modified such that an unlabeled compound was added in excess to determine whether it behaves as a competitive inhibitor of the initial transport rate. While these assays do not definitively prove transport of the competitive inhibitor, they do suggest an interaction between a putative substrate and a transport system (such as allosteric inhibition). The putative inhibitors tested were fosphomycin (a potent inhibitor of *E. coli* G3P transport [30]), triose phosphates, and other small sugar molecules individually added in 20-fold excess of the estimated apparent K_t for G3P or DHAP (from Fig. 2A and B, respectively). Figure 5 shows that only triose phosphate compounds resulted in measurable inhibition of [^{14}C]G3P or [^{32}P]DHAP uptake. Thus, we postulate that *R. prowazekii* possesses a broad substrate specificity triose phosphate transport system(s) similar to that previously shown for plant plastids (31–33). The observed differences in the estimated apparent K_i (kinetic constant of inhibition) of the inhibitory triose phosphates again suggest the presence of more than one *R. prowazekii* G3P and DHAP transport system (Fig. 5, K_i values given below each compound label on the abscissa). For example, DHAP inhibited [^{14}C]G3P transport with an estimated K_i of ~218 μM, an affinity that is substantially different from the estimated apparent K_t for DHAP transport (~6 μM). If the two substrates share a single carrier-mediated transport system (with a single substrate binding site), then K_i should approach K_t. In addition, the inhibition profiles observed for DHAP and G3P appear distinct in that glycerol-2-phosphate and phosphoenol pyruvate inhibited the rate of G3P transport to a much greater extent than that of DHAP. Although suggestive of at least two distinct transport systems, the data presented here do not ultimately rule out the existence of a single transporter that displays stark differences in substrate recognition/binding and mechanism of action depending on the substrate. These inhibition data also raise the possibility that glyceraldehyde-3-phosphate, 3-phosphoglycerate,

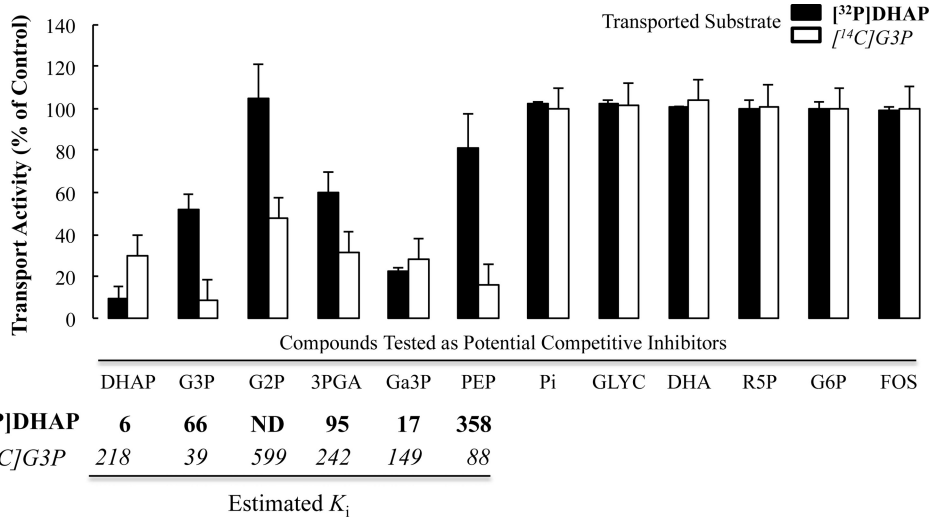

FIG 5 G3P and DHAP substrate specificity profiles in purified *R. prowazekii*. Initial linear rates of transport of [^{14}C]G3P (20 μM) and [^{32}P]DHAP (10 μM) in the absence or presence of candidate substrates were determined with purified *R. prowazekii* suspended in modified SPGMg^{2+} buffer at 34°C. Data points are presented for each time point as a percentage of the rate of either G3P or DHAP transport in the absence of any other candidate substrate. The data shown are averages of technical triplicates of at least three independent rickettsial preparations. The substrate specificity of the G3P and DHAP transport systems was assayed by testing putative candidate substrates to determine if they behave as competitive inhibitors of either G3P or DHAP transport. Each putative candidate substrate was added at a concentration of 20 times the reported K_t of each for G3P (K_t, ~40 μM) and DHAP (K_t, ~6 μM). For each candidate substrate that displayed inhibition of either G3P or DHAP transport, a K_i was estimated by an algebraic manipulation of the modified Michaelis-Menten equation for determining velocity in the presence of an inhibitor $\{v_i = (V_{max}[S])/([S] + K_m(1 + ([I]/K_i)^{-1}$, where [S] is the substrate concentration and [I] is the inhibitor concentration} and reported in the table below the corresponding data in italic font for G3P and bold font for DHAP. Error bars represent the standard deviations of the means. Abbreviations: ND, not determined; G2P, glycerol-2-phosphate; 3PGA, 3-phosphoglycerate; Ga3P, glyceraldehyde-3-phosphate; Pi, inorganic phosphate; GLYC, glycerol; DHA, dihydroxyacetone; R5P, ribose-5-phosphate; G6P, glucose-6-phsophate; FOS, fosfomycin.

and glycerol-2-phosphate are transported by *R. prowazekii* despite the fact that annotated enzymes required to metabolize these substrates are not present (3, 6, 34). A detailed analysis of the eukaryotic host cell metabolome in response to rickettsial infection will make it possible to discern whether triose phosphate concentrations in the host cell cytoplasm dictate whether or not they are available for transport. Together, our observations speak to a loose-fitting substrate-binding site in the *R. prowazekii* G3P and DHAP transporters and open the intriguing possibility that changing concentrations of other host triose phosphate pools regulates the influx of G3P and DHAP.

DISCUSSION

The studies presented here are the first description of mechanistic and energetic properties of the triose phosphate transport systems used by the obligate intracellular pathogen *R. prowazekii*. On the basis of the data, we posit the existence of multiple *R. prowazekii* triose phosphate transport systems that exhibit diversity with respect to kinetics, energetics, mechanisms of action, and substrate specificity profiles. Considering that *R. prowazekii* has no endogenous source of G3P for phospholipid synthesis, these transport systems are likely critical to intracellular growth. This point raises interesting questions regarding the links between intracellular growth and pathogenesis (35) and rickettsial phospholipase A (PLA) activity. When the host cell is encountered and entered, a PLA is activated and PLA activity increases concomitant with the increasing numbers of rickettsiae until the host cell eventually lyses (36). Despite this constitutive PLA activity, the host cell does not lyse until it is literally full of rickettsiae, indicating that a critical mass of microbes is required for the cell lysis facet of pathogenesis. Perhaps dual rickettsial transporter systems function in concert to maintain a growth rate ultimately required for host cell lysis. Moreover, these dual transport systems may also function to increase the rate of host cell resource depletion, which ultimately impairs the host cell's ability to repair damage caused by the constitutive PLA activity, thus contributing to lysis. This raises the provocative concept that *R. prowazekii* triose phosphate acquisition systems represent metabolic virulence factors that contribute to pathogenesis. Whether the G3P and DHAP transport systems are functionally redundant, are differentially regulated and work individually, or must work in combination to supply triose phosphates to fuel rickettsial growth and drive pathogenesis are interesting questions yet to be resolved.

Our previous study of *R. prowazekii* triose phosphate metabolism was the first to describe a bacterial DHAP transport system (18). Until that report, DHAP transport systems had been characterized in organelles such as plant plastids and trypanosome glycosomes (28, 37, 38). Our present study has added a layer of complexity to this story with respect to a noted difference in the observed mechanisms of DHAP transport. The plastidic DHAP transporters function by using a phosphate-dependent obligate exchange antiport mechanism where the addition of a counter-substrate to the medium is essential to elicit intracellular substrate efflux (31, 33, 39). Conversely, the *R. prowazekii* DHAP transport system exhibits little substrate efflux regardless of transport assay reaction buffer composition. It is possible that the observed low rate of radiolabel efflux was due to the conversion of DHAP to G3P, although this was not directly assessed.

We previously reported that DHAP transported over the time course tested is >80% intact by chromatographic analysis (18); thus, there is a limited possibility that DHAP is metabolized to a

compound that itself is not available for efflux from the rickettsial cell. With that caveat stated, it is tempting to speculate that the *R. prowazekii* DHAP transport system uses a bona fide uniport mechanism reminiscent of the Pit phosphate transporter of *E. coli* where substrate moves in only one direction through the transport system, into the cell cytosol (40, 41). Also similar to the *E. coli* Pit system, the *R. prowazekii* DHAP transport system appears to require PMF to generate a substrate concentration gradient and accumulate cytoplasmic DHAP. Identification of the *R. prowazekii* DHAP transporter(s) is required to fully determine the mechanism of action and whether this system represents a new family of bacterial triose phosphate transporters.

We have previously discussed an *R. prowazekii* homologue of the bacterial G3P/inorganic phosphate obligate exchange antiporter, GlpT (42), as a possible triose phosphate transporter and described our difficulties in assaying its activity in *E. coli* because of overexpression toxicity (18). However, our energetic and mechanistic studies here suggest that the observed rickettsial transport of G3P cannot be ascribed only to a putative *R. prowazekii* GlpT. In fact, the observed ATP dependence of *R. prowazekii* G3P transport is more reminiscent of the *E. coli* Ugp ABC-type transport system (43). While no Ugp homologues are identifiable in the *R. prowazekii* genome, there are several candidate ABC-type transporters that have yet to be assigned a functional role (6). Further studies are required to determine which of the rickettsial ABC-type transporters play roles in G3P transport.

The complex nature of *R. prowazekii* triose phosphate acquisition exemplifies the fascinating interplay between a eukaryotic host cell and a parasite—two organisms competing for the same, limited pool of metabolites required for growth. Indeed, redundancy and metabolic flexibility appear critical even in the face of reductive evolution (1). As we begin to better understand the eukaryotic host cell metabolome and the attendant effects of *R. prowazekii* infection, so too will we better grasp the exerted selective pressures that have maintained multiple triose phosphate transport systems.

While the inherent selective advantages of maintaining differentially regulated, independent metabolic pathways that adapt to an ever-changing environment are patent, a more perplexing question is how the loss of metabolic versatility also provides a selective advantage. Part of the answer may perhaps lie in an unknown role for rickettsial transporters as regulators of the intracellular growth rate. *R. prowazekii* grows with a generation time of ~10 h despite the fact that eukaryotic cell cytoplasm is a nutrient-rich environment (3, 35). Slow growth may be advantageous by preserving the human host growth niche in order to maximize the odds that a louse vector will take a blood meal, ingest the pathogen, and disseminate it. Reliance on transporters to fulfill metabolic requirements may facilitate instantaneous regulation (or fine tuning) of *R. prowazekii* growth based on the bioavailability of host cell substrates.

The paradigm of transport, slow growth, and rickettsial pathogen-host interactions must also integrate the complex regulatory potential of changing host cell triose phosphate pools. We observed that glyceraldehyde-3-phosphate, 3-phosphoglycerate, and glycerol-2-phosphate behave as inhibitors of G3P and DHAP transport. Thus, rickettsial growth and pathogenesis will depend not only on changes in host G3P and DHAP pools but also on the kinetic effects associated with changes in the concentrations of other triose phosphates that behave as competitive transport inhibitors. The fact that triose phosphates other than G3P and DHAP may be transported by rickettsiae but cannot presumably be metabolized raises interesting questions regarding possible regulatory effects of "dead-end substrates" on rickettsial cytosolic metabolism.

In the end, the obligate intracytosolic bacterium *R. prowazekii* has optimally balanced the selective advantages of genome reduction and the maintenance of metabolic flexibility. The concept of transport systems that function as metabolic virulence factors to effectively parasitize the host may be key to our understanding of the evolutionary interplay between rickettsiae and their host. Identification of the *R. prowazekii* G3P and DHAP transport systems will facilitate studies of gene regulation and generation of gene knockouts to further our understanding of triose phosphate transport systems within the context of the ever-changing host cell metabolome in response to infection.

ACKNOWLEDGMENTS

We are indebted to Herb Winkler for his numerous insights into the work presented here. We also thank Nicole Housley, Rosemary Roberts, Mary Patton, Michael Housley, and Robin Daugherty for technical assistance. Additional thanks go to David Wood and John Foster for critical reading of the manuscript.

This work was supported by Public Health Service grant R21 AI-069210 from the National Institute of Allergy and Infectious Diseases to J.P.A.

The content of this report is solely our responsibility and does not necessarily represent the official view of the NIAID or NIH.

REFERENCES

1. **Audia JP.** 2012. Rickettsial physiology and metabolism in the face of reductive evolution, p 221–242. *In* Palmer GH, Azad AF (ed), Intracellular pathogens II: *Rickettsiales*. ASM Press, Washington, DC.
2. **Hackstadt T.** 1996. The biology of rickettsiae. Infect. Agents Dis. **5:**127–143.
3. **Winkler HH.** 1990. *Rickettsia* species (as organisms). Annu. Rev. Microbiol. **44:**131–153.
4. **Valbuena G, Feng HM, Walker DH.** 2002. Mechanisms of immunity against rickettsiae. New perspectives and opportunities offered by unusual intracellular parasites. Microbes Infect. **4:**625–633.
5. **Valbuena G, Walker DH.** 2009. Infection of the endothelium by members of the order *Rickettsiales*. Thromb. Haemost. **102:**1071–1079.
6. **Andersson SGE, Zomorodipour A, Andersson JO, Sicheritz-Pontén T, Alsmark UCM, Podowdki RM, Naslund AK, Eriksson A-S, Winkler HH, Kurland CG.** 1998. The genome sequence of *Rickettsia prowazekii* and the origin of mitochondria. Nature **396:**133–140.
7. **Andersson JO, Andersson SG.** 1999. Insights into the evolutionary process of genome degradation. Curr. Opin. Genet. Dev. **9:**664–671.
8. **Andersson JO, Andersson SGE.** 1999. Genome degradation is an ongoing process in *Rickettsia*. Mol. Biol. Evol. **16:**1178–1191.
9. **Andersson SGE, Kurland CG.** 1998. Reductive evolution of resident genomes. Trends Microbiol. **6:**263–268.
10. **Smith DK, Winkler HH.** 1977. Characterization of a lysine-specific active transport system in *Rickettsia prowazekii*. J. Bacteriol. **129:**1349–1355.
11. **Winkler HH.** 1976. Rickettsial permeability: an ADP-ATP transport system. J. Biol. Chem. **251:**389–396.
12. **Winkler HH, Daugherty RM.** 1986. Acquisition of glucose by *Rickettsia prowazekii* through the nucleotide intermediate uridine 5′-diphosphoglucose. J. Bacteriol. **167:**805–808.
13. **Audia JP, Winkler HH.** 2006. Study of the five *Rickettsia prowazekii* proteins annotated as ATP/ADP translocases (Tlc): Only Tlc1 transports ATP/ADP, while Tlc4 and Tlc5 transport other ribonucleotides. J. Bacteriol. **188:**6261–6268.
14. **Atkinson WH, Winkler HH.** 1989. Permeability of *Rickettsia prowazekii* to NAD. J. Bacteriol. **171:**761–766.
15. **Tucker AM, Winkler HH, Driskell LO, Wood DO.** 2003. *S*-Adenosylmethionine transport in *Rickettsia prowazekii*. J. Bacteriol. **185:**3031–3035.

16. **Zahorchak RJ, Winkler HH.** 1983. Transmembrane electrical potential in *Rickettsia prowazekii* and its relationship to lysine transport. J. Bacteriol. **153:**665–671.
17. **Cai J, Winkler HH.** 1996. Transcriptional regulation in the obligate intracytoplasmic bacterium *Rickettsia prowazekii*. J. Bacteriol. **178:**5543–5545.
18. **Frohlich KM, Roberts RA, Housley NA, Audia JP.** 2010. *Rickettsia prowazekii* uses an *sn*-glycerol-3-phosphate dehydrogenase and a novel dihydroxyacetone phosphate transport system to supply triose phosphate for phospholipid biosynthesis. J. Bacteriol. **192:**4281–4288.
19. **Walker TS, Winkler HH.** 1979. Rickettsial hemolysis: rapid method for enumeration of metabolically active typhus rickettsiae. J. Clin. Microbiol. **9:**645–647.
20. **Winkler HH, Lehninger AL.** 1968. The atractyloside-sensitive nucleotide binding site in a membrane preparation from rat liver mitochondria. J. Biol. Chem. **243:**3000–3008.
21. **Perlin DS, Latchney LR, Senior AE.** 1985. Inhibition of *Escherichia coli* H^+-ATPase by venturicidin, oligomycin and ossamycin. Biochim. Biophys. Acta **807:**238–244.
22. **Daugherty RM, Linka N, Audia JP, Urbany C, Neuhaus HE, Winkler HH.** 2004. The nucleotide transporter of *Caedibacter caryophilus* exhibits an extended substrate spectrum compared to the analogous ATP/ADP translocase of *Rickettsia prowazekii*. J. Bacteriol. **186:**3262–3265.
23. **Winkler HH, Miller ET.** 1978. Phospholipid composition of *Rickettsia prowazekii* grown in chicken embryo yolk sacs. J. Bacteriol. **136:**175–178.
24. **Tzianabos T, Moss CW, McDade JE.** 1981. Fatty acid composition of rickettsiae. J. Clin. Microbiol. **13:**603–605.
25. **Winkler HH.** 1976. Rickettsial cell water and membrane permeability determined by a micro space technique. Appl. Environ. Microbiol. **31:**146–149.
26. **Rosen BP.** 1971. Basic amino acid transport in *Escherichia coli*. J. Biol. Chem. **246:**3653–3662.
27. **Auer M, Kim MJ, Lemieux MJ, Villa A, Song J, Li XD, Wang DN.** 2001. High-yield expression and functional analysis of *Escherichia coli* glycerol-3-phosphate transporter. Biochemistry **40:**6628–6635.
28. **Quick WP, Neuhaus HE.** 1996. Evidence for two types of phosphate translocators in sweet-pepper (*Capsicum annum* L.) fruit chromoplasts. Biochem. J. **320**(Pt 1):7–10.
29. **Maloney PC.** 1994. Bacterial and plant antiporters. J. Exp. Biol. **196:**439–442.
30. **Elvin CM, Hardy CM, Rosenberg H.** 1985. Pi exchange mediated by the GlpT-dependent *sn*-glycerol-3-phosphate transport system in *Escherichia coli*. J. Bacteriol. **161:**1054–1058.
31. **Fliege R, Flugge UI, Werdan K, Heldt HW.** 1978. Specific transport of inorganic phosphate, 3-phosphoglycerate and triosephosphates across the inner membrane of the envelope in spinach chloroplasts. Biochim. Biophys. Acta **502:**232–247.
32. **Heldt HW, Flugge UI, Borchert S.** 1991. Diversity of specificity and function of phosphate translocators in various plastids. Plant Physiol. **95:**341–343.
33. **Neuhaus HE, Wagner R.** 2000. Solute pores, ion channels, and metabolite transporters in the outer and inner envelope membranes of higher plant plastids. Biochim. Biophys. Acta **1465:**307–323.
34. **Coolbaugh JC, Progar JJ, Weiss E.** 1976. Enzymatic activities of cell-free extracts of *Rickettsia typhi*. Infect. Immun. **14:**298–305.
35. **Winkler HH.** 1995. *Rickettsia prowazekii*, ribosomes and slow growth. Trends Microbiol. **3:**196–198.
36. **Winkler HH, Daugherty RM.** 1989. Phospholipase A activity associated with the growth of *Rickettsia prowazekii* in L929 cells. Infect. Immun. **57:**36–40.
37. **Borchert S, Harborth J, Schunemann D, Hoferichter P, Heldt HW.** 1993. Studies of the enzymic capacities and transport properties of pea root plastids. Plant Physiol. **101:**303–312.
38. **Fairlamb AH, Opperdoes FR.** 1986. Carbohydrate metabolism in African trypanosomes, with special reference to the glycosome, p 183–224. *In* Morgan MJ (ed), Carbohydrate metabolism in cultured cells. Plenum Publishing Corporation, New York, NY.
39. **Batz O, Scheibe R, Neuhaus HE.** 1992. Transport processes and corresponding changes in metabolite levels in relation to starch synthesis in barley (*Hordeum vulgare L.*) etioplasts. Plant Physiol. **100:**184–190.
40. **Beard SJ, Hashim R, Wu G, Binet MR, Hughes MN, Poole RK.** 2000. Evidence for the transport of zinc(II) ions via the pit inorganic phosphate transport system in *Escherichia coli*. FEMS Microbiol. Lett. **184:**231–235.
41. **Rosenberg H, Gerdes RG, Harold FM.** 1979. Energy coupling to the transport of inorganic phosphate in *Escherichia coli* K12. Biochem. J. **178:**133–137.
42. **Huang Y, Lemieux MJ, Song J, Auer M, Wang DN.** 2003. Structure and mechanism of the glycerol-3-phosphate transporter from *Escherichia coli*. Science **301:**616–620.
43. **Su TZ, Schweizer HP, Oxender DL.** 1991. Carbon-starvation induction of the ugp operon, encoding the binding protein-dependent sn-glycerol-3-phosphate transport system in *Escherichia coli*. Mol. Gen. Genet. **230:**28–32.